

# Laser-induced scanning tunneling microscopy: Linear excitation of the junction plasmon

Joonhee Lee, Shawn M. Perdue, Desiré Whitmore, and V. Ara Apkarian<sup>a)</sup>

*Department of Chemistry, University of California, Irvine, California 92697-2025, USA*

(Received 20 July 2010; accepted 26 August 2010; published online 14 September 2010)

We introduce the cross-polarized double-beat method for localized excitation of the junction plasmon of a scanning tunneling microscope with femtosecond laser pulses. We use two pulse trains derived from a Ti:sapphire laser operating at a repetition frequency of  $f_s=76$  MHz, with a relative shift between their carrier frequencies  $\omega_a/2\pi=f_s+f_b$  controlled with an acousto-optic modulator. The trains are cross-polarized and collinearly focused on the junction, ensuring constant radiation flux. The anisotropic susceptibility of the junction plasmon mixes the fields, which modulate the tunneling current at  $f_b$  (the difference between carrier beat and repetition frequency) at base-band frequencies that can be used for direct detection of the tunneling current. The interferometric cross-correlation of the pulses and the polarization dependence of the mixing identify the coupling to the radiation to be through the coherent  $z$ -displacement of the tip plasmon. Single Ag atoms are used to demonstrate microscopy under irradiation. In the linear coupling regime, the laser-induced displacement of the plasmon is operationally indistinguishable from the mechanical displacement of the junction gap. © 2010 American Institute of Physics. [doi:10.1063/1.3490398]

The goal of combining scanning tunneling microscopy (STM) with ultrafast spectroscopy to reach the angstrom femtosecond space-time limit of relevance to molecular science has been long pursued.<sup>1-5</sup> Although there have been significant developments,<sup>6-9</sup> including methods such as photoconductivity gated STM,<sup>10,11</sup> the promise of imaging with submolecular spatial resolution on femtosecond timescales remains unfulfilled. To clock events, the method must involve nonlinear optics (multiple short pulses); and to retain the spatial resolution of the STM, one of the optical steps must involve photoinjection of a tunneling electron with a short laser pulse. Efforts in this regard have had limited success, principally due to thermal artifacts.<sup>12-14</sup> To be useful for imaging purposes, displacements of the junction must be maintained to a tolerance of  $\delta z < 10^{-3}$  Å, which is a challenge under conditions of pulsed irradiation. A particular challenge is the detection of laser-induced tunneling (LIT) current at electron injection rates that fall within the gain-bandwidth product of current amplifiers ( $<10$  kHz at picoampere sensitivity) without amplitude modulation of radiation because such low frequencies lead to thermal oscillations of the junction gap.<sup>15</sup> Another challenge is to localize the excitation to the tip apex, the active area of which ( $\sim 10$  nm) is much smaller than the diffraction limit of light. There have been several approaches to accomplish the latter aim while minimizing the heat load on the junction: superfocusing with sharp tips,<sup>16</sup> waveguiding tips,<sup>17</sup> and waveguiding substrates<sup>18</sup> are among the examples. Here, we introduce the cross-polarized double-beat method that relies on the frequency modulation of femtosecond pulse trains and linear mixing by the anisotropic susceptibility of the junction

plasmon.<sup>19</sup> The method allows localization of the modulated excitation to the junction plasmon while maintaining a steady heat load. We limit the presentation to the weak-field, linear coupling regime, where photoinduced tunneling with femtosecond laser pulses can be demonstrated with mechanical displacements of the junction maintained below  $10^{-3}$  Å. Using an atomically sharp Ag tip to probe Ag adatoms on metal surfaces, we demonstrate LIT imaging and compare the results to mechanical  $z$ -modulation of the junction gap. Extension of the method to the strong field limit (where ionization harmonics and the generation of attosecond electron pulse trains can be observed) is taken up separately.<sup>20</sup>

## I. DOUBLE-BEAT METHOD

The experimental setup is shown in Fig. 1. The output of a Ti:sapphire laser is actively intensity stabilized to within 0.05%, then passed through an acousto-optic modulator (AOM). The undiffracted beam and the first order diffracted beam form two pulse trains

$$\vec{E}_1(t) = \sum_n \varepsilon(t - nT) \hat{\varepsilon}_1 \exp[i(kr - \omega_o t)], \quad (1a)$$

$$\vec{E}_2(t) = \sum_n \varepsilon(t - nT) \hat{\varepsilon}_2 \exp[i(kr - (\omega_o + \omega_a)t)], \quad (1b)$$

with a difference in their carrier frequencies  $\omega_a$ , controlled by the rf driver of the AOM. The pulse trains are cross-polarized and recombined in a Mach-Zehnder interferometer and then focused on the STM junction through a plano-convex lens of focal length = 10 cm, with an estimated spot size at the junction of  $\sim 50$  μm. A half-wave plate is used to rotate the cross-polarized pair, to impinge at  $\pm \pi/4$  relative to the tip, which is taken to lie along the  $z$ -axis (see inset in Fig. 1)

<sup>a)</sup> Author to whom correspondence should be addressed. Electronic mail: aapkaria@uci.edu.

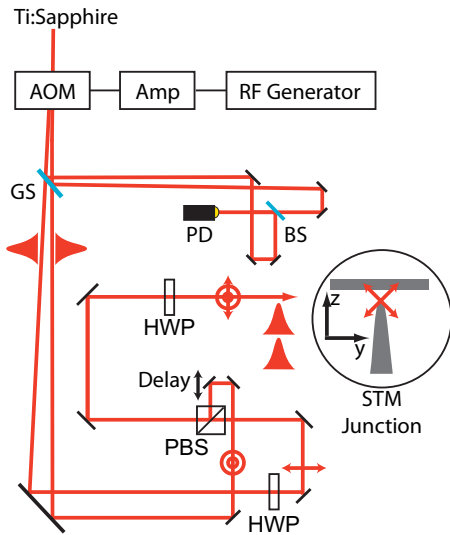


FIG. 1. Schematic of the optical setup. AOM: acousto-optical modulator, Amp: radio-frequency amplifier with a 40 dB gain, GS: glass slide, BS: beam splitter, PD: photodiode, PBS: polarizing cube beam splitter, and HWP: half-wave plate. The cross-polarized pulse pair impinges at  $\pm 45^\circ$  relative to the tip, as shown in the inset.

$$\hat{\epsilon}_1 = \frac{(\hat{z} + \hat{y})}{\sqrt{2}}, \quad \hat{\epsilon}_2 = \frac{(\hat{z} - \hat{y})}{\sqrt{2}}. \quad (2)$$

A small fraction of the beams is picked off to form the reference double-beat interferometer (Fig. 1). The signal generated on the reference photodiode is the carrier beat  $\omega_a$ , sampled with the pulse train

$$I_{\text{ref}}(t) = c \sum_n \varepsilon^2(t - nT) [1 + \cos(\omega_a t)] \quad (3)$$

in which  $\varepsilon(t)$  is the pulse envelope of the femtosecond pulses and the sampling rate  $f_s = 1/T = 76$  MHz is given by the repetition rate of the laser. The power spectrum of the sampled wave consists of the harmonic comb at the harmonics of sampling frequency and sidebands

$$I_{\text{ref}}(f) = \sum_m a_{m,n} \delta[f - (mf_s + nf_a)], \quad (4)$$

$$m = 0, 1, 2, \dots; \quad n = 0, \pm 1,$$

in which  $|f_s - f_a| \equiv f_b$  corresponds to the beat between the envelope and carrier beat. The reference beat can also be generated electronically by mixing the output of a monitor photodiode and the rf driver. A feedback loop in which the rf is adjusted can be used to lock the carrier envelope phase of the pulse train,<sup>21</sup> which becomes valuable in nonlinear mixing applications in the strong field limit.

The cross-polarization of the pulse trains ensures that the radiation flux reaching the junction is constant. In isotropic media, such as the cubic crystals of Ag (fcc) or W (bcc) used to fabricate the STM tip, the linear susceptibility is strictly diagonal ( $\chi_{ii}^{(1)}$ ); therefore, the pulse trains do not interfere

$$P^{(1)}(t)^2 = |\chi_{11}^{(1)}|^2 E_1^2(t) + |\chi_{22}^{(1)}|^2 E_2^2(t) = \sigma(I_1(t) + I_2(t)). \quad (5)$$

This is verified using a square law detector, which shows interference strictly due to the limited extinction ( $10^{-3}$ ) of the polarizing beam splitter. At a laser repetition rate of 76

MHz, the thermal expansion of the tip reaches a steady state [on the timescale of  $\sim 10$  min at cryogenic temperatures, under ultra-high vacuum (UHV) conditions]. In contrast, the anisotropic susceptibility of the plasmon at the STM junction,<sup>22</sup>  $\chi_{zz}^{(1)} > \chi_{xx}^{(1)} = \chi_{yy}^{(1)}$ , mixes the fields through the induced polarization. Now, the  $z$ -components of the applied fields beat in phase with the reference interferometer

$$|P_z(t, \omega_b)|^2 = \sigma_z(\hat{\epsilon}_1 \cdot \hat{z})(\hat{\epsilon}_2 \cdot \hat{z})[E_1(t)E_2^*(t) + E_1^*(t)E_2(t)]. \quad (6)$$

The scheme allows arbitrary control of the modulation frequency of the tip plasmon. Thus, for a laser repetition rate of 76 MHz, choosing a rf of 76 MHz–1 kHz, the  $m=1$ , and  $n=-1$  components in Eq. (4) occur at  $f_b=1$  kHz (at base band). Lock-in detection of the tunneling current isolates the photoinjected electrons. Note that the role of the anisotropic susceptibility of the tip apex is to rotate polarization: when there is constructive interference along the  $z$ -axis, destructive interference happens along the  $y$ -axis and vice versa. The net radiation intensity at the tip is constant.

The experiments are carried out in a home-built STM, with relevant design parameters that have been described previously.<sup>23</sup> The measurements are made at 5 K under UHV conditions (base pressure of  $4 \times 10^{-11}$  torr). The junction we study consists of Ag atoms adsorbed on either a Ag(110) or a NiAl(110) surface and an atomically sharp Ag tip. The plasmon resonance of such a junction, which we observe through electroluminescence, is a broad peak that overlaps the Ti:sapphire spectrum. The laser power used in these experiments is in the range of 4–10 mW focused down to a spot diameter of 50  $\mu\text{m}$ .

## II. RESULTS AND ANALYSIS

In Fig. 2 we show the interferometric cross-correlation of pulses, recorded over a silver atom, by detecting the tunneling current as a function of delay  $\tau$  between the two pulse trains. The measurements are carried out in the tunneling regime, at a dc current set point of 0.5 nA corresponding to a junction gap of 6  $\text{\AA}$ . A lock-in amplifier, locked to the double-beat frequency of the reference interferometer, is used. The LIT current follows the optical phase

$$S(\tau) \propto e^{-\tau^2/2\Delta t^2} \cos(2\pi f_b \tau - \omega_o \tau), \quad (7)$$

with modulation at the optical carrier frequency of the Ti:sapphire laser (375 THz, 800 nm), as verified by the Fourier transform of the signal shown in Fig. 2. The pulsewidth at the junction is 60 fs. The interference signal, over zero background (Fig. 2), confirms that the signal is strictly due to the cross term between the pulse trains [Eq. (6)].<sup>24</sup> The detected tunneling current is only possible as an outcome of the interference between the coherent cross-polarization of the tip plasmon at optical frequencies  $P(\omega_o)P^*(\omega_o + \omega_a) + \text{c.c.}$  and with instantaneous response. Instead of rectification,<sup>25</sup> it is the polarization that is modulated at  $\omega_a$ , a frequency too high for any thermomechanical response of the junction.

The polarization dependence of the LIT current as a function of the rotation angle  $\varphi$  of the 1/2-wave plate is

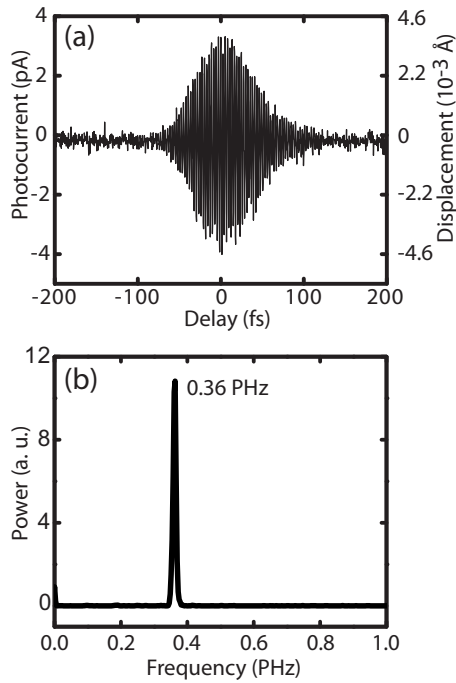


FIG. 2. (a) Cross-correlation current using lock-in detection at the double-beat frequency. The measurement was carried out with the tip placed above a Ag atom adsorbed on NiAl(110), with STM current feedback turned off (except for periodic tracking tests to ensure that the entire measurement is recorded at the same position). The left ordinate represents the observed current, while the right ordinate is the current equivalent displacement of the junction gap obtained from a calibration of the  $z$ -piezo response. (b) The Fourier transform of the cross-correlation shows the optical carrier frequency; the polarization response is instantaneous.

shown in Fig. 3. The angular dependence of the current reveals mixing purely along the  $z$ -component of the fields, as in Eq. (6)

$$I(\varphi) \propto (\hat{\epsilon}_1 \cdot \hat{z})(\hat{\epsilon}_2 \cdot \hat{z}) = \cos(\varphi - \pi/4)\cos(\varphi + \pi/4) = \frac{\cos(2\varphi)}{2}. \quad (8)$$

The perfect reproduction of the angular dependence through Eq. (8) separately establishes that the interferometric tunneling current is entirely the result of linear mixing of the cross-polarized fields. The phase-locked current can be understood as the coherent displacement of the plasmon, i.e., modulation of the collective electron density of the tip. As illustrated schematically in Fig. 3(b), observables associated with the displacement of the plasmon are indistinguishable from the mechanical displacement of the junction gap [Fig. 3(c)]. The current equivalent mechanical  $z$ -displacement of the tip, shown on the right ordinate of Fig. 2, is  $\sim 10^{-3}$  Å; any thermal contribution to the modulation of the tip must be smaller than this limit.

The more demanding test of LIT microscopy is imaging with atomic resolution. In Fig. 4, we show images of a Ag atom on a Ag(110) surface. In Fig. 4(a), we show the constant current topographic image of the silver atom. The identical image is obtained whether the junction is irradiated or not. The LIT image recorded by tracing the topographic contour [Fig. 4(b)] does not show any contrast on the adatom (at each pixel, the feedback is turned off and the modulated

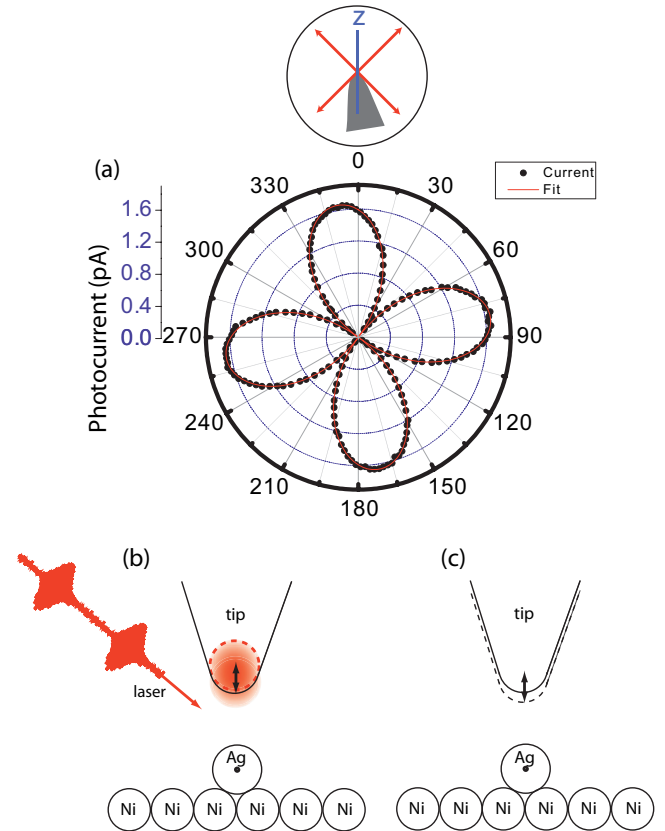


FIG. 3. (a) The polarization dependence of the laser-induced tunneling current shows that it is the anisotropic linear susceptibility that mixes the cross-polarized pulse trains. The LIT current is plotted as a function of the angle between the tip and the crossed pair. The angle is  $0^\circ$  when the crossed pair polarizations are at  $\pm 45^\circ$  relative to the laboratory  $z$ -axis. A  $9^\circ$  tilt of the tip with respect to the laboratory  $z$ -axis is extracted from the fit to Eq. (8), which assumes mixing through the  $z$ -dipole of the tip plasmon. [(b) and (c)] Schematic of plasmon displacement versus mechanical displacement of the tip. Both effects lead to the same change in the tunneling probabilities. The principle distinction between these two processes is in the response time. While the plasmon modulation follows the optical phase frequency (Fig. 2), the thermomechanical response time of the tip and substrate are much slower. The tip shaft is  $\sim 10$  Hz, tip apex is  $\sim 1$  kHz, and surface is  $\sim 100$  kHz, determined by thermal diffusivity and geometry (Ref. 15).

current is recorded). In contrast, in constant height mode imaging, the dc current [Fig. 4(c)] and the modulated LIT current [Fig. 4(d)] yield the same image. It is verified that this LIT image disappears when the cross-polarized pulses do not overlap in time [Fig. 4(e)]. These observations are consistent with the effect of the laser being strictly  $z$ -modulation of the tip plasmon, which is verified by reproducing the constant height mode LIT image with constant height mode  $z$ -modulation imaging [Fig. 4(f)]. As another demanding test of the method, we consider the librational spectrum of CO adsorbed on the same surface.<sup>26</sup> The spectrum shown in Fig. 4(g), obtained as a  $d^2I/dV^2$  curve with the bias modulated at 200 Hz, is perfectly reproduced while irradiating the junction (double-beat frequency of 1 kHz). There is no cross-talk between the two modulations; no discernible thermal artifact.

### III. CONCLUSIONS

The cross-polarized double-beat method enables LIT microscopy void of thermal artifacts. The cross-correlation of

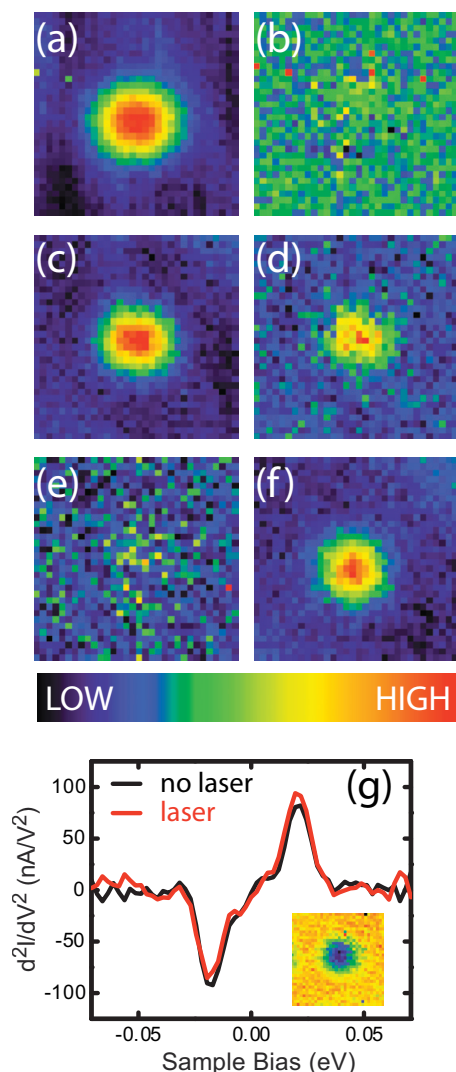


FIG. 4. Laser-induced tunneling images of Ag atoms on Ag(110) surface. (a) Topography at 0.2 nA, 2 V, and (b) simultaneously acquired LIT image in constant current mode. The laser modulation frequency is 1 kHz and the incident laser power is 10 mW. (c) Topography and (d) LIT image obtained at 0.2 nA, 2 V in constant height mode. (e) LIT image obtained when the two pulses do not overlap in time. (f)  $dI/dz$  image obtained at 0.12 nA, 2 V. The tip piezo modulation frequency is 400 Hz, the modulation amplitude is  $6 \times 10^{-3}$  Å. (g) A comparison of vibrational spectrum of a single CO molecule under laser illumination (red) and without the laser illumination (black). The inset is the topography of the single CO molecule on which the spectra were recorded.

the femtosecond pulse trains, the polarization dependence of the LIT current, and the LIT images identify coherent modulation of the tip plasmon as the mechanism of the observed LIT microscopy at 800 nm. Operationally, in imaging applications, coherent modulation of the collective surface electron density is indistinguishable from the mechanical dis-

placement of the junction gap. In the present linear limit, the radiation modulates the tunneling probability. For ultrafast imaging applications, it is essential that an electron be injected within the laser pulse. To this end, it is essential to resort to the strong field limit, which we consider in the follow-up paper.

## ACKNOWLEDGMENTS

This research was made possible through the NSF Center for Chemical Innovation dedicated to Chemistry at the Space-Time Limit (Grant no. CHE-0802913). We are grateful for Professor W. Ho's guidance in the construction of the STM used in these measurements. We acknowledge the fruitful discussions with A. Rodriguez Perez during the course of this work.

- <sup>1</sup>R. J. Hamers and D. G. Cahill, *Appl. Phys. Lett.* **57**, 2031 (1990).
- <sup>2</sup>W. Pfeiffer, F. Sattler, S. Vogler, G. Gerber, J. Y. Grand, and R. Möller, *Appl. Phys. B: Lasers Opt.* **64**, 265 (1997).
- <sup>3</sup>V. Gerstner, A. Knoll, W. Pfeiffer, A. Thon, and G. Gerber, *J. Appl. Phys.* **88**, 4851 (2000).
- <sup>4</sup>S. Grafström, *J. Appl. Phys.* **91**, 1717 (2002).
- <sup>5</sup>M. Merschtorf, W. Pfeiffer, A. Thon, and G. Gerber, *Appl. Phys. Lett.* **81**, 286 (2002).
- <sup>6</sup>H. Shigekawa, O. Takeuchi, and M. Aoyama, *Sci. Technol. Adv. Mater.* **6**, 582 (2005).
- <sup>7</sup>O. Takeuchi, M. Aoyama, R. Oshima, Y. Okada, H. Oigawa, N. Sano, H. Shigekawa, R. Morita, and M. Yamashita, *Appl. Phys. Lett.* **85**, 3268 (2004).
- <sup>8</sup>D. Riedel, C. Delacour, A. J. Mayne, and G. Dujardin, *Phys. Rev. B* **80**, 155451 (2009).
- <sup>9</sup>P. A. Sloan, *J. Phys.: Condens. Matter* **22**, 264001 (2010).
- <sup>10</sup>K. Takeuchi and Y. Kasahara, *Appl. Phys. Lett.* **63**, 3548 (1993).
- <sup>11</sup>N. Khusnatdinov, T. J. Nagle, and G. Nunes, *Appl. Phys. Lett.* **77**, 4434 (2000).
- <sup>12</sup>P. I. Geshev, S. Klein, and K. Dickmann, *Appl. Phys. B: Lasers Opt.* **76**, 313 (2003).
- <sup>13</sup>J. Boneberg, M. Tresp, M. Ochmann, H.-J. Münzer, and P. Leiderer, *Appl. Phys. A: Mater. Sci. Process.* **66**, 615 (1998).
- <sup>14</sup>V. Gerstner, A. Thon, and W. Pfeiffer, *J. Appl. Phys.* **87**, 2574 (2000).
- <sup>15</sup>S. Grafström, J. Kowalski, R. Neumann, O. Probst, and M. Wörtge, *J. Vac. Sci. Technol. B* **9**, 568 (1991).
- <sup>16</sup>Kh. V. Nerkararyan, *Phys. Lett. A* **237**, 103 (1997).
- <sup>17</sup>C. Ropers, C. C. Neacsu, T. Elsaesser, M. Albrecht, M. B. Raschke, and C. Lienau, *Nano Lett.* **7**, 2784 (2007) and references therein.
- <sup>18</sup>E. Verhagen, L. Kuipers, and A. Polman, *Nano Lett.* **7**, 334 (2007).
- <sup>19</sup>O. J. F. Martin and C. Girard, *Appl. Phys. Lett.* **70**, 705 (1997).
- <sup>20</sup>J. Lee, S. M. Perdue, A. Rodriguez Perez, and V. A. Apkarian (unpublished).
- <sup>21</sup>S. Koke, C. Grebing, H. Frei, A. Anderson, A. Assion, and G. Steinmeyer, *Nat. Photonics* **4**, 462 (2010).
- <sup>22</sup>N. Behr and M. B. Raschke, *J. Phys. Chem. C* **112**, 3766 (2008).
- <sup>23</sup>B. C. Stipe, M. A. Rezaei, and W. Ho, *Rev. Sci. Instrum.* **70**, 137 (1999).
- <sup>24</sup>J.-C. Diels and W. Rudolph, *Ultrashort Laser Pulse Phenomena* (Academic, San Diego, 1996).
- <sup>25</sup>A. V. Bragas, S. M. Landi, and O. E. Martinez, *Appl. Phys. Lett.* **72**, 2075 (1998).
- <sup>26</sup>H. J. Lee and W. Ho, *Science* **286**, 1719 (1999).